


INFE-241-RI/41

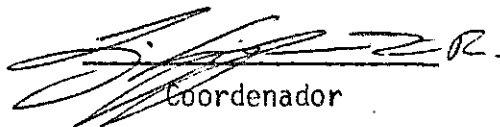
PROJETO: MESA

TÍTULO: THEORETICAL ANALYSIS OF LEE WAVES
OVER THE ANDES AS SEEN BY SATELLITE
PICTURES

AUTOR (ES): R. P. Sarker e R. V. Calheiros

PUBLICADO EM: Setembro 1972



Gerente do Projeto

Coordenador

THEORETICAL ANALYSIS OF LEE WAVES OVER THE ANDES

AS SEEN BY SATELLITE PICTURES

by

R.P. Sarker* and R.V. Calheiros**

Instituto de Pesquisas Espaciais (INPE)

São José dos Campos, SP - Brasil

ABSTRACT

Satellite pictures have been utilised to detect mountain waves on the lee of the Andes range. The wavelengths as observed in the pictures from the distribution of clouds in parallel bands lie between 20 to 30 kms for the five cases examined. The wavelengths have also been computed theoretically for these cases by an analytical method and a quasi-numerical method, using linearised perturbation equations. Wavelengths so computed are fairly in good agreement with the observed wavelengths. Vertical velocities associated with the waves along the different sectors of the Andes have also been computed. Their maximum values are of the order of 1 to 5 m sec⁻¹. Also the quasi-stationary character of the waves, as noticed in some of the pictures, is discussed.

* On leave from India Meteorological Department

**Also from Fundação Educacional de Bauru, S.P., Brasil

1. INTRODUCTION

During the last two decades the problem of mountain wave has engaged the attention of many theoretical meteorologists in different parts of the world. Of these, mentions may be made of Scorer (1949), Queney (1947) Palm and Foldvik (1960), Sawyer (1960), Döös (1961), Krishnamurti (1964), Sarker (1965), Pekelis (1966,69), Onishi (1969), Vergeiner (1971) etc., Of the recent observational studies mention may be made of those of Kuettner and Lilly (1968) and Vergeiner and Lilly (1970) over the Colorado Rockies. The advent of satellite photography has opened up a new dimension to the observational problem of mountain waves. The typical orographic clouds, which appear on the lee side of a mountain, in parallel bands, can be beautifully recorded by Satellite Cameras. These pictures lend an added support to the evidence of existence of lee waves under favorable meteorological conditions. Few authors, e.g. Döös (1962), Conover (1964), Fritz (1965), Cohen et al (1967), De (1970) have utilised the satellite cloud pictures to detect mountain waves and to measure their wavelengths. Döös (1962) made a case study of mountain wave over the Andes mountains utilising a Tiros I picture. Fritz (1965) used Tiros V and Tiros VI pictures to study the same problem in different mountaineous regions. Of the four cases reported by him one was for the Andes mountains. Cohen et al (1967) used Tiros VIII pictures to study mountain waves in the Middle East in four cases. De (1970) utilised ESSA 3 pictures to examine the same problem in the Assam hills in East India for sixteen cases.

But for the two cases mentioned above, one by Döös and another by Fritz, we are not aware of any study, observational or theoretical,

on the same problem over the Andes mountains. In this paper we present five cases of mountain waves over the different sectors of the Andes mountains. For the evidence of these waves we have used ITOS-1, NIMBUS-3 and ATS-3 satellite pictures. The wavelengths as measured from these pictures have been compared with those computed theoretically. For theoretical computation we have made use of two methods - an analytical method used by Sarker (1965), Palm and Foldvik (1960), Döös (1961) and a quasi-numerical method used by Sawyer (1960) and Sarker (1967). We have also computed the vertical velocities associated with the waves for the different cross-sections of the Andes mountains, where the waves were actually observed. The quasi-stationary character of the waves which has been noticed in some of the pictures is also discussed. We may point out here that we have not presented any new theory in this paper, but have tried to examine if the satellite cloud pictures support the validity of the existing theories on the subject.

2. SATELLITE PICTURES AND THE QUASI-STATIONARY CHARACTER OF WAVES:

The satellite pictures utilised in this study for the evidence of mountain waves were obtained from the National Oceanic and Atmospheric Administration and also a picture (NIMBUS-3) received by the APT station of the Brazilian Space Research Institute was used. Figures 1, 2, 4, 5 show the pictures from ITOS-1 heliosynchronous satellites and Fig. 3 shows the picture from NIMBUS-3 satellite. These are the pictures from where the wavelengths have been measured with which are compared

the theoretically computed wavelengths. The time and orbit of these pictures and the area of location of the waves are given in Table 1. It should be mentioned here that in the case of ITOS pictures, a half-degree allowance in latitude must be given in the location of the lee waves due to gridding errors and 10% allowance for the measured wavelengths must be considered due to inaccuracies in the determination of wave crests, picture distortion and imperfect alignment of the cloud rows. In the case of NIMBUS-3 picture the gridding error can be between 0.5 to 1° of latitude because of the gridding process available and a 10% allowance for wavelength must be kept. In each of these cases an average wave axis was found by analysing the whole area of interest and an average wavelength was calculated by measuring the distance and the number of waves in the lee wave area. The wavelengths so measured are given in Table 1. Caution must be exercised when comparing these values with the theoretically computed values, because of the limitations mentioned above.

It would be seen from Table 1 that the time of these pictures is about 20 G.M.T. except the NIMBUS-3 picture which was taken at about 16 G.M.T. For our theoretical computation we could get only 12 G.M.T. meteorological data. How far it would be justified depends on the quasi-stationary character of the waves. We could examine this aspect in four out of the five cases with the help of the pictures obtained by the ATS-3 geosynchronous space craft. The time of these pictures and the wavelengths obtained from these pictures are given in Table 1. We have not reproduced

these pictures here, but we have verified that the areas of location of the lee waves in these pictures almost coincide with those given by the ITOS-1 pictures. It may be, however, noted that for the ATS-3 pictures gridding error is more because of the satellite orbital plane oscillations and wavelength allowance should be increased to about 15% because of poorer resolution and larger distortion as compared to the near-polar orbit satellites. Perhaps due to these reasons we get slightly smaller values of wavelengths from ATS-3 pictures in all these cases. The difference in time of photograph is another important factor. However, it is quite clear from the comparison of the two sets of pictures that the lee waves maintained nearly the same characteristics in shape, location and wavelength for a period of about eight hours at least. Because of this quasi-stationary character of the waves we feel we are justified to base our theoretical computation on available 12 G.M.T. meteorological data and compare the results with the pictures obtained about 8 hours later, which are more reliable than the ATS-3 pictures.

3. THEORETICAL TREATMENT

The theoretical treatment that is being presented here involves the following assumptions:

- (i) The motion is two dimensional in the vertical xz -plane with z -axis vertical and x -axis directed eastward along the undisturbed current \bar{U} . The airstream blows perpendicularly to the ridge which is considered to have an infinite extent

along north-south direction;

- (ii) Undisturbed quantities, wind \bar{U} , temperature \bar{T} , density $\bar{\rho}$ are functions of z only;
- (iii) The motion is steady, frictionless and laminar;
- (iv) The characteristic scale of the motion is so small that effect of earth's rotation can be neglected and
- (v) Perturbation technique is utilised. Perturbation quantities are small so that their product and higher order terms can be neglected compared to the undisturbed quantities.

On these assumptions the linearised equation for the perturbation vertical velocity w is given by (see Palm and Foldvik 1960, Döös 1961, Sarker 1965)

$$\frac{\partial^2 w_1}{\partial x^2} + \frac{\partial^2 w_1}{\partial x^2} + f(z) w_1 = 0 \quad (3.1)$$

where

$$f(z) = \frac{g(v^* - v)}{\bar{U}^2 \bar{T}} - \frac{1}{\bar{U}} \frac{d^2 \bar{U}}{dz^2} + \left(\frac{v^* - v}{\bar{T}} - \frac{g}{X \bar{R} \bar{T}} \right) \frac{1}{\bar{U}} \frac{d\bar{U}}{dz} - \frac{2}{X \bar{R} \bar{T}} \left(\frac{d\bar{U}}{dz} \right)^2 - \left(\frac{g - Rv}{2 \bar{R} \bar{T}} \right)^2 \quad (3.2)$$

and

$$w = w_1 \exp \left(\frac{g - Rv}{2 \bar{R} \bar{T}} z \right) \approx w_1 \left(\frac{\bar{\rho}_0}{\bar{\rho}_z} \right)^{\frac{1}{2}} \quad (3.3)$$

The equation (3.1) is analogous to that of Palm and Foldvik (1960) and Döös(1961).

In the above

$\bar{U}, \bar{T}, \bar{\rho}$ undisturbed wind, temperature and density respectively.

$\bar{\rho}_0, \bar{\rho}_z$ values of $\bar{\rho}$ at surface and height z .

g acceleration due to gravity.

γ^* adiabatic lapse rate, dry or moist.

γ actual lapse rate in the undisturbed atmosphere
 $= - \frac{d\bar{T}}{dz}$

R gas constant for unit mass.

$\chi = \frac{g}{g - R\gamma}$ which is equal to $\frac{c_p}{c_v}$, ratio of specific heats at constant pressure and constant volume, for dry adiabatic lapse rate.

Equation (3.1) is solved subject to two boundary conditions.

The condition at the ground requires that the mountain itself is a streamline so that motion is tangential to the mountain surface. The upper boundary condition requires that the energy of the wave remains finite at great heights. With these conditions equation (3.1) is solved both analytically and numerically.

3.1 ANALYTICAL METHOD

Equation (3.1) can be solved analytically if the function $f(z)$, defined by (3.2), which is a function of stability, wind speed and wind shear of the undisturbed atmosphere, can be represented analytically. If we can represent $f(z)$ by

$$f(z) = f(0) e^{-2\tilde{c}z}$$

or

$$\ell^2(z) = \ell_0^2 e^{-2cz} \quad (3.1.1)$$

the equation (3.1) reduces to a Bessel eq. [Palm and Foldvik (1960), Döös (1961), Sarker (1965)] and if the mountain is represent by a bell-shaped profile

$$\zeta(x) = \frac{a^2 b}{a^2 + x^2} \quad \text{at } z = 0 \quad (3.1.2)$$

where "b" is the height of the mountain and "a" is the half-width where the height is b/2, then the solution of the vertical velocity is given by

$$w(x, z) = w_p + w_r \quad (3.1.3)$$

with

$$w_r = - \bar{U}(0) 2 \pi a b \exp \left(\frac{g - Rv}{2 R \bar{T}} \right) \sum_{k=1}^n (e^{-akn} k_n \cos k_n x) \times$$

$$\times \frac{J_{m_n}(\beta e^{-cz})}{\frac{d}{dk} J_{m_n}(\beta)} \quad \text{for } x > 0$$

$$= 0 \quad \text{for } x < 0 \quad (3.1.4)$$

$$\left. \begin{aligned} \text{Where } \beta &= \frac{f_0^{\frac{1}{2}}}{c} = \frac{\ell(0)}{c} \\ m &= \frac{k}{c} \end{aligned} \right\} \quad (3.1.5)$$

In the above k is the wave number. The wave numbers k_1, k_2 , etc are obtained from the positive roots m_1, m_2, \dots of the equation

$$J_m(\beta) = 0 \quad (3.1.6)$$

J_m being the Bessel function of first kind. For $f(z)$ Scorer (1949) used the parameter ℓ^2 . The term w_r is the vertical velocity due to the lee wave. The term w_p is important only in the vicinity of the mountain and dies away rapidly with increasing $|x|$ and has different expressions for positive and negative x . Instead of using the equation (3.1.6) wavelengths can be easily calculated with the help of the nomograms given in Fig. 6a, b, c knowing the values of ℓ_0 and c .

3.2 QUASI-NUMERICAL METHOD

Analytical solution of equation (3.1) becomes difficult if the function $f(z)$ cannot be represented by an analytical function like (3.1.1) and the solution can be obtained by numerical method only. Sawyer (1960) obtained numerical solution of equation (3.1) for arbitrary distribution of $f(z)$ by assuming that $f(z) = \text{constant} = L$ above a certain height $z = z_1$. We call this method a "quasi-numerical method", as the mountain is still

represented by a bell-shaped profile defined by (3.1.2). Sarker (1967) followed a similar method and computations were made easier by taking $L = 0.0 \text{ km}^{-2}$, as the choice of L has only very small effect at low levels [Palm and Foldvik (1960), Corby and Sawyer (1958), Sawyer (1960)]. Then the solution for vertical velocity becomes [Sarker (1967)]

$$w(x,z) = \left(\frac{\bar{\rho}_0}{\bar{\rho}_2}\right)^{\frac{1}{2}} \bar{U} [\zeta(x)]^* R_e [x_1 + x_2 + x_3] \quad (3.2.1)$$

where R_e means the real part and

$$x_3 = -2\pi \sum \frac{\psi(z, k_r)}{\psi'(0, k_r)} k_r \quad \text{ab} \quad \exp(-ak_r + ik_r x) \quad \text{for } x > 0$$

$$= 0 \quad \text{for } x < 0$$

and

$$\psi'(0, k_r) = \left[\frac{d}{dk} \psi(0, k) \right]_k = k_r \quad (3.2.2)$$

x_3 is the vertical velocity for the lee wave. The terms x_2 and x_3 are important near the mountain. x_1 has an expression valid for all x and x_2 has different expressions for positive and negative x . k_r is the lee wave number. The variation of the undisturbed velocity along the mountain profile is provided in (3.2.1) through $\bar{U} [\zeta(x)]$. To obtain the numerical solution the values of $\psi(z, k_r)$ are required at different levels and for different values of k and so also is required the value of $\psi'(0, k_r)$. For fixed values of k , values of $\psi(z, k)$ for different levels are obtained by the difference equation

$$\psi_{r-1} = -\psi_{r+1} + [2 - d^2(f_r - k^2)]\psi_r \quad (3.2.3)$$

with the boundary conditions

$$\left. \begin{aligned} \psi_N &= 1 & \text{at } z &= z_1 \\ \psi_{N-1} &= 1 + \frac{k^2 d^2}{2} + kd \end{aligned} \right\} \quad (3.2.4)$$

where integration is started at level $z = z_1$ and d is the finite difference interval of 0.25 km. Values of $\psi'(0, k)$ are obtained by solving a similar finite difference equation obtained by differentiating equation (3.2.3) with respect to k subject to the boundary conditions obtained by differentiating the relations (3.2.4). The lee wave is given by the singularity of the function $\frac{\psi(z, k)}{\psi(0, k)}$. The preliminary zeros are obtained from the alternating signs of $\psi(0, k)$ calculated for 32 values of k in the range 0 to 5 km^{-1} . These preliminary zeros are used as starting points for an iterative Newton-Raphson method to locate the zeros of $\psi(0, k)$ which give the lee waves.

4. COMPUTATION AND DISCUSSION

The lee waves were observed in different sectors of the Andes Mountains. The average mountain profiles along these sectors are given in Figures 7 a, b, c, d. In each figure the dashed line represents the actual average profile and the solid line represents the idealised bell-shaped profile given by

$$\eta(x) = \frac{a^2 b}{a^2 + x^2} \quad \text{at } z = h$$

where h is the height of the average ground level in the area. Values of the parameters a , b , h for the different cases are given in Table 1.

To compute the wavelength theoretically, we require the vertical distribution of undisturbed wind and temperature on the windward side of the mountain in the neighbourhood of the region where waves were actually observed in the satellite pictures. But in this respect we are in a serious handicapped position. The network of radiosonde stations in South America is really very sparse. As a result we were constrained to take available wind and temperature data from stations that are not located in the best place in relation to the mountain wave area. Figures 8 a through 12 a represent wind and temperature profiles for the five cases studied and figures 8 b through 12 b represent the corresponding $f(z)$ profiles. Each diagram represents data from a station which is not very near the area of wave observation and sometimes data from 2 stations were pooled together to construct a realistic profile.

In Case 1 (1 January, 1971) waves were observed in the area $47^{\circ} - 49^{\circ}\text{S}$, $69^{\circ} - 72^{\circ}\text{W}$. Meteorological data up to 700 mb were taken from Neuquen Aero ($37-715$, $38^{\circ}57'\text{S}$, $68^{\circ}08'\text{W}$), Argentina and data above 700 mb were taken from Don Torcuato Aero ($37-568$, $34^{\circ}29'\text{S}$, $58^{\circ}37'\text{W}$), Argentina. In case 2 (12 December 1970) waves were observed near $41.5^{\circ} - 42.5^{\circ}\text{S}$, $68 - 72^{\circ}\text{W}$. In this case data up to 400 mb were from Neuquen Aero and data above 400 mb were taken from Mendoza Observatorio ($37 - 420$, $32^{\circ}53'\text{S}$, $68^{\circ}51'\text{W}$), Argentina. In case 3 (25 February 1970) waves were observed in the region $40 - 46^{\circ}\text{S}$, $66 - 72^{\circ}\text{W}$. In this case surface data were taken from

Rawinsonde Station Puerto Montt (85-801, $41^{\circ}28'S$, $72^{\circ}56'W$), Chile and upper air data were taken from Neuquen Aero.

In case 4 (6 January 1971) waves were observed in the region $42^{\circ} - 44^{\circ}S$, $70 - 72^{\circ}W$. In this case data up to 400 mb were taken from Neuquen Aero and data above were taken from Quintero (85-543, $32^{\circ}50'S$, $71^{\circ}32'W$), Chile. Surface data were not available. In case 5 (2 February 1971) waves were observed in the region $42.5^{\circ} - 44.5^{\circ}$, $67 - 70^{\circ}W$. Meteorological data in this case were taken from Neuquen Aero. In each case some smoothing was necessary to construct a realistic profile. We have used 12 GMT data in all the cases. This is not a serious objection because of the quasi-stationary character of the waves discussed earlier.

We are very much aware of the limitations of the meteorological data we have used. One may have serious objections to use data from a station which is quite far away from the place of wave observation. But these are the best available data we could lay our hands on.

Examination of Figures 8(a) through 12(a) will show that wind and temperature are favourably distributed for wave formation, namely, wind generally increases with height and the atmosphere has stable stratification. The $f(z)$ profile generally decreases with height [Fig. 8(b) - 12(b)]. According to Scorer (1949), for waves that are normally observed $f(z)$ should decrease sufficiently with height. This, however, need not necessarily always be the case.

By taking the actual values of $f(z)$ above the general ground level at an interval of 0.5 km we have computed wavelength by the quasi-numerical method in all the five cases and they are given in Table 1. In three cases we computed wavelength by analytical method also, where $f(z)$ could be represented by an exponential function defined by (3.1.1). Of course exponential representation was not very satisfactory. So for comparison with observed wavelengths we shall give more weightage to the wavelengths computed by the quasi-numerical method. The wavelengths computed by the analytical method are slightly more than those computed by numerical method (Table 1).

For comparison we shall be concerned with the longest computed wavelengths. We have verified that the shorter computed waves give very little amplitudes for the different mountain profiles we have considered and are, therefore, of little interest to us. For example, the magnitudes of vertical velocities for shorter waves are at least two orders of magnitude less than the vertical velocities for the longer waves. We see that the computed longer wavelengths are quite in good agreement with the observed wavelengths in all the cases. We have already mentioned the uncertainties involved in estimating the observed wavelengths. Uncertainties are also involved in computed wavelengths due to a number of factors. The stations from which we were forced to take meteorological data were not ideally situated in relation to the mountain wave area. They were situated quite far away. This fact definitely casts some doubt on the accuracy of the computed wavelengths. The height of the mean general ground level above the sea level is also another important factor. The choice of this height h is a bit subjective.

We have assumed the 12 G.M.T. meteorological data to be representative of the conditions of about 20 G.M.T. when the pictures were taken. For wavelengths computed by the analytical method, another cause of uncertainty lies in the idealised representation of the $f(z)$ profile, which we found was not quite satisfactory. In spite of the inaccuracies involved in both the observed and computed wavelengths, we get good agreement in all the cases and therefore, it would be reasonable to state that the cases presented here support the validity of the two theories we have used.

We have computed vertical velocities associated with the waves for the different cross-sections of the mountains where the waves were actually observed. For this purpose we used the wavelengths computed by the quasi-numerical method. The variations of the amplitudes of vertical velocity with height are shown in Figures 13 a - 13e, for the different cases. It would be seen that there are one or two reversals of phases and the velocity then decreases with height. This suggests that there are one or two cellular motions below the motion of external type above. The maximum vertical velocity in each case is given in Table 1. It is of the order of 1 to 5 m sec^{-1} .

5. CONCLUSIONS

Following conclusions may be drawn from this study:

- i) The airstream in the Andes mountains appears to have favourable wind distribution and stable stratification to give rise to mountain waves during the months December to February, at least for the cases examined here.

- ii) The wavelengths as observed in the satellite pictures vary between 20 to 30 km. They are found to be quasi-stationary.
- iii) Wavelengths computed by the theoretical methods are in good agreement with the observed wavelengths, in spite of the inaccuracies involved in computed and measured wavelengths. This supports the validity of the theoretical methods used here.
- iv) The vertical velocities associated with the lee waves are of the order of 1 to 5 m sec⁻¹.
- v) Associated with the waves one or two cellular motions exist below the motion of external type above.

6. ACKNOWLEDGEMENT

We are thankful to Dr. Fernando de Mendonça, General Director and Dr. Luiz Gylvan Meira Jr., Scientific Director, INPE, for supporting this work and for the facilities they have kindly provided. We also thank Mr. Walton Follansbee and Mr. L.F. Whitney, Jr., NOAA, for supplying us the ITOS and ATS satellite pictures. Thanks are also due to Miss Maria Regina Soares who typed the manuscript.

REFERENCES

1. Cohen, A. and Doron, E. 1967 "Mountain lee waves in the Middle East: Theoretical Calculations compared with satellite Pictures" J. App. Meteor. vol. 6, pp 669-673.
2. Conovar, J.H. 1964 "The identification and significance of orographically induced clouds observed by TIROS Satellites". J. App. Meteor. vol. 3, pp 226-234.
3. Corby, A. and Sawyer, J. S. 1958 "The airflow over a ridge: The effects of the upper boundary and high level conditions" Quart. J. Roy. Meteor. Soc. vol. 84, pp. 25- 37.
4. De, U.S. 1970 "Lee waves as evidenced by Satellite cloud Pictures", I.J. Met.Geophy. vol. 21, No 4, pp. 637 - 647.
5. Döös, B.R. 1961 "A mountain wave theory including the effect of wind and stability" Tellus vol. 13, pp. 305 - 319.
6. Döös, B.R. 1962 "A Theoretical analysis of lee wave clouds observed by TIROS I". Tellus, vol. 14. pp. 301 - 309

- | | | | |
|-----|--------------------------------|------|--|
| 7. | Fritz, S. | 1965 | "The significance of mountain lee waves as seen from satellite pictures". <u>J. App. Meteor.</u> vol. 4 pp. 31 - 37. |
| 8. | Krishnamurti, T.N. | 1964 | "The finite amplitude mountain wave problem with entropy as a vertical co-ordinate".
<u>Month- Weather - Review</u> , vol. 92, n° 4., pp 147 - 160. |
| 9. | Kuettner, J.P. and Lilly, D.K. | 1968 | "Lee waves in the Colorado Rockies" <u>Weatherwise</u> , vol. 21, pp. 180 - 196. |
| 10. | Onishi, G. | 1969 | "A numerical method for three-dimensional mountain waves" <u>J. Met. Soc. Japan</u> , vol. 47, pp. 352 - 359. |
| 11. | Palm, E. and Foldvik, A. | 1960 | "Contribution to the Theory of two-dimensional mountain waves" <u>Geof. Publ.</u> vol. 21, n° 6, 30 pp. |
| 12. | Pekelis, E.M. | 1966 | "A numerical calculation of finite-amplitude orographic disturbances (the two-dimensional problem)" <u>Izv. Atm. Oceanic Phy.</u> vol. 2 pp. 1113 - 1125. |
| 13. | Pekelis, E.M. | 1969 | "A numerical method of calculating lee waves with an arbitrary distribution of the basic flow parameters (two-dimensional linear problem)" <u>Izv. Atm. Oceanic Phy.</u> vol. 5 pp. 3 - 16 |

14. Queney, P. 1947 "Theory of Perturbations in stratified currents with application to airflow over mountain barriers" The Univer. Chicago Press, Misc. Rep. n° 23.
15. Sarker, R.P. 1965 "A theoretical study of mountain waves on Western Ghats". I.J. Meteor. Geophy. vol. 16, pp. 565 - 584.
16. Sarker, R. P. 1967 "Some modifications in a dynamical model of orographic rainfall". Month Weather Review, vol. 95 n° 10, pp. 673 - 684.
17. Sawyer, J.S. 1960 "Numerical Calculation of the displacements of a stratified airstream crossing a ridge of small height". - Quart. J.R. Meteor. Soc. vol. 86, pp 326 - 345.
18. Scorer, R.S. 1949 "Theory of waves in the lee of mountains", Quart. J.R. Meteor. Soc., vol. 75, pp 41 - 56.
19. Vergeiner, I. and Lilly, D.K. 1970 "The dynamic structure of lee wave flow as obtained from balloon and airplane observations" Month- Waath- Review, vol. 98 pp. 220 - 232.

20. Vergeiner, I. 1971 "An operational linear lee wave model for arbitrary basic flow and two-dimensional topography", Quart. J.R. Meteor. Soc., vol. 97, pp. 30 - 60.

LEGEND OF THE DIAGRAMS

FIG. 1 - ITOS 1 AVCS picture, orbit 4295, January 1st 1971, 20:06:59 GMT

FIG. 2 - ITOS 1 AVCS picture, orbit 4045, December 12th 1970, 20:30:30 GMT

FIG. 3 - NIMBUS 3 APT picture, February 25th, 1970, 16:16:00 GMT

FIG. 4 - ITOS 1 AVCS picture, orbit 4358, January 6th 1971, 20:59:25 GMT

FIG. 5 - ITOS 1 AVCS picture, orbit 4696, February 2nd 1971, 21:24:22 GMT

FIG. 6 - Nomogram to find wavelength directly from values of ℓ_0 and c ,
defined by $f(z) = \ell^2(z) = \ell_0^2 e^{-2cz}$ (equation (3.1.1.)

(a) If a point (ℓ_0, c) falls on the left of the line $L_1 = \infty$, there
is no wave. If it falls between $L_1 = \infty$ and $L_2 = \infty$ there is
one wave

(b) Two waves for points between $L_2 = \infty$ and $L_3 = \infty$

(c) Three waves for points between $L_3 = \infty$ and $L_4 = \infty$.

Four or more waves for points on the right of $L_4 = \infty$

FIG. 7 - Average mountain profiles. Dashed line represents actual profile.

Solid line represents idealised bell-shaped profile given by

$$\zeta(x) = \frac{a^2 b}{a^2 + x^2} \quad \text{at } z = h.$$

- (a) Profile along latitude 48°S . For the bell-shaped profile
 $a = 10 \text{ km}$, $b = 0.6 \text{ km}$, $h = 0.75 \text{ km}$ (case 1)
- (b) Profile along latitude 42°S . For bell-shaped profile $a = 10 \text{ km}$,
 $b = 0.5 \text{ km}$, $h = 1.0 \text{ km}$ (case 2)
- (c) Profile along latitude 43°S . For bell-shaped profile $a = 10 \text{ km}$,
 $b = 0.6 \text{ km}$, $h = 0.9 \text{ km}$ (cases 3 and 4).
- (d) Profile along latitude 43.5° . For bell-shaped profile $a = 13 \text{ km}$
 $b = 0.7 \text{ km}$, $h = 0.8 \text{ km}$ (case 5).

FIG. 8 (a) - Wind and temperature profiles for 1 January 1971.

(b) - $f(z)$ profile for 1 January 1971.

FIG. 9 (a) - Wind and temperature profiles for 12 December 1970.

(b) - $f(z)$ profile for 12 December 1970.

FIG. 10 (a) - Wind and temperature profiles for 25 February 1970.

(b) - $f(z)$ profile for 25 February 1970.

FIG. 11 (a) - Wind and temperature profiles for 6 January 1971.

(b) - $f(z)$ profile for 6 January 1971

FIG. 12 (a) - Wind and temperature profiles for 2 February 1971.

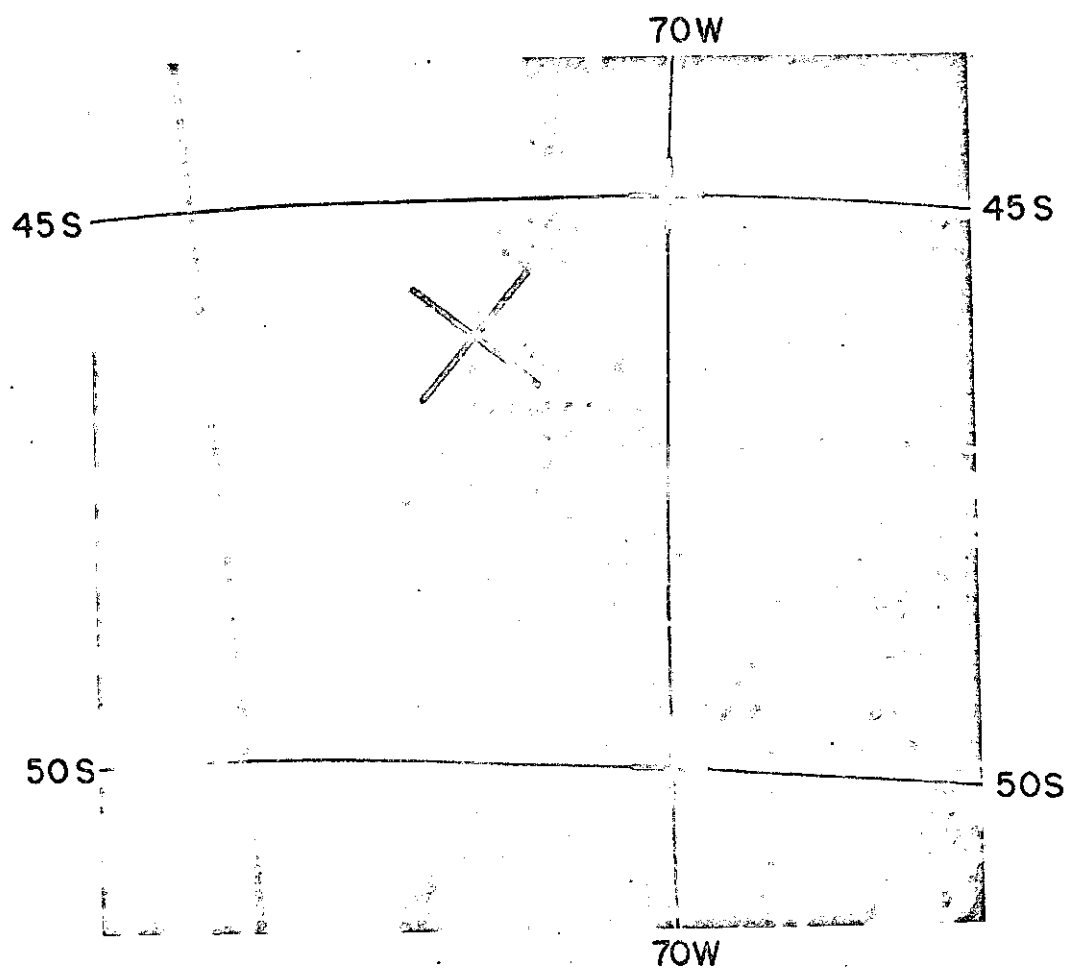
(b) - $f(z)$ profile for 2 February 1971.

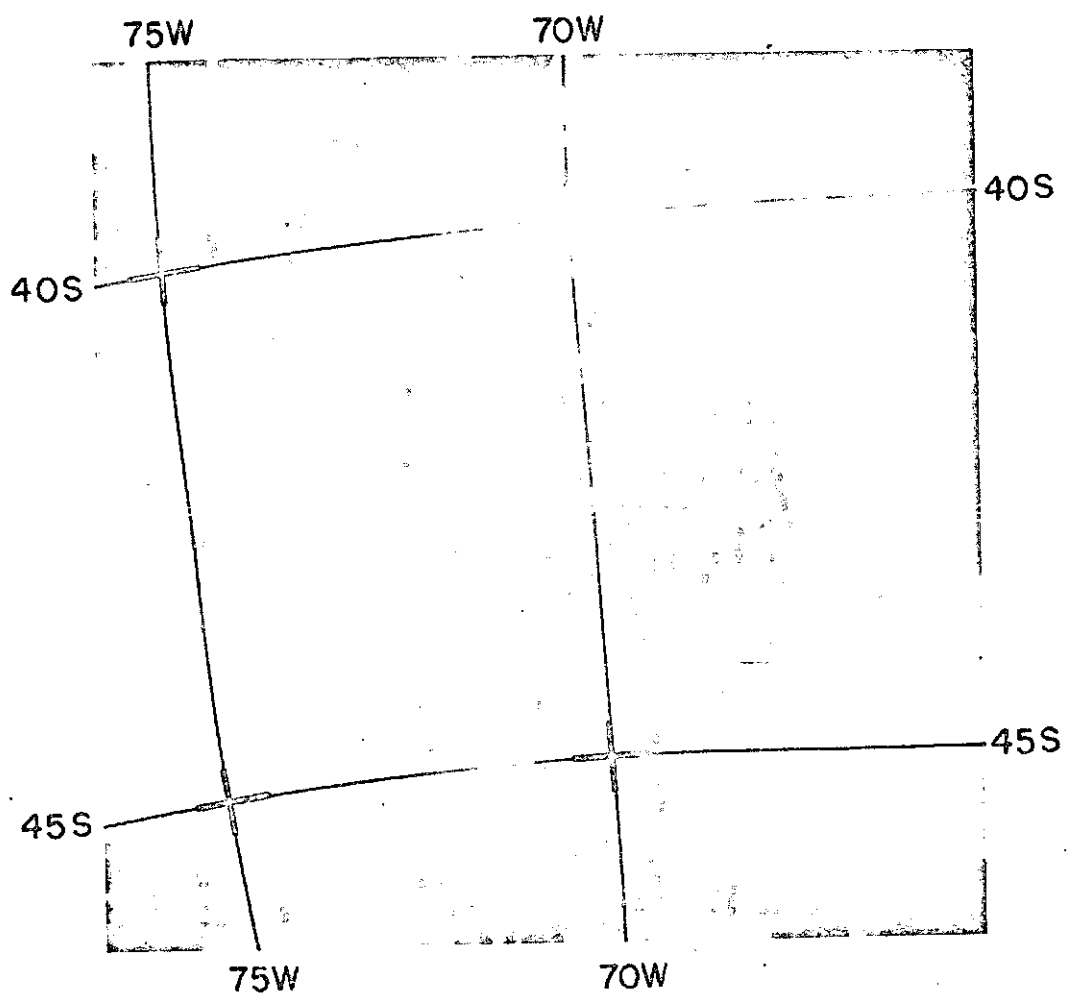
FIG. 13 - Variation of vertical velocity $[x_3$ of equ (3.2.2) for $\cos k_r x = 1$] with height.

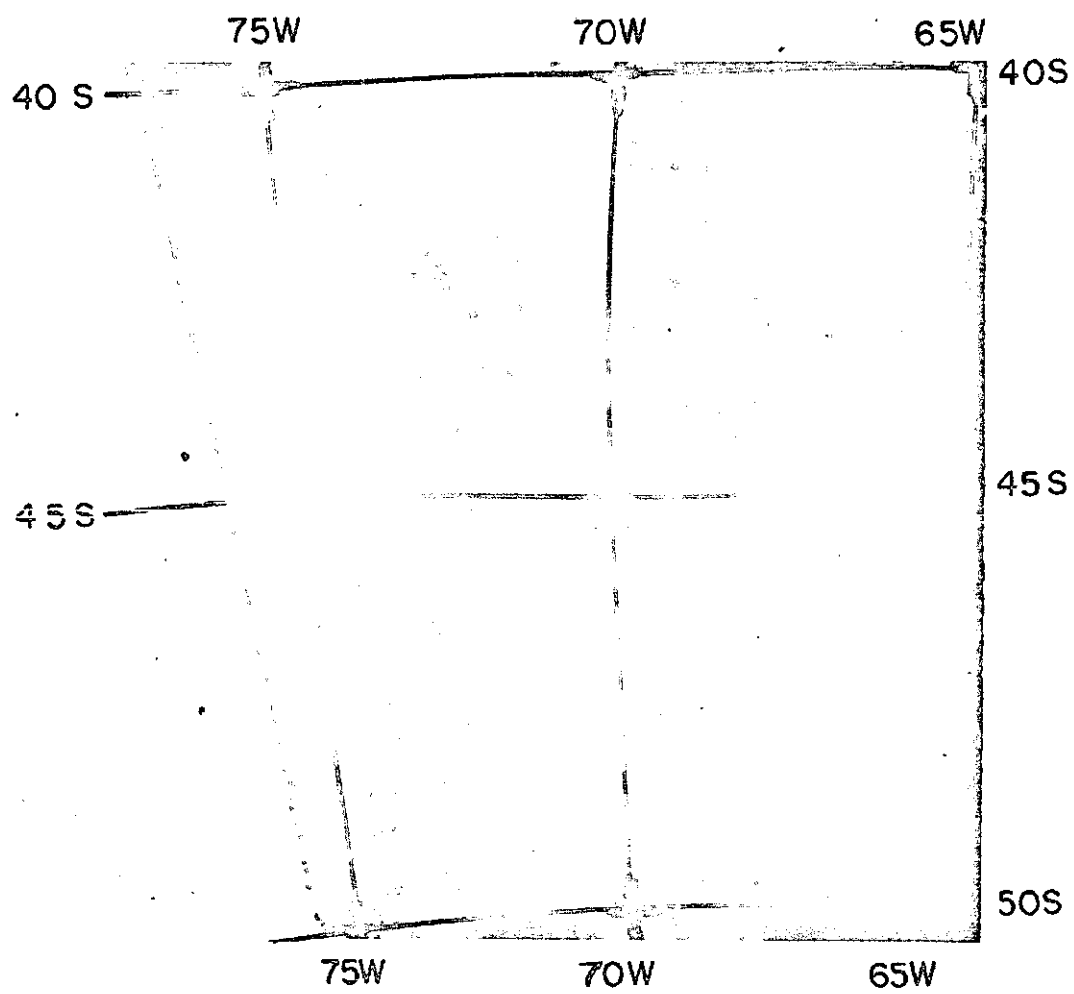
- (a) 1 January 1971. $L = 19.1$ km . $a = 10$ km, $b = 0.6$ km along 48°S
- (b) 12 December 1970. $L = 18.0$ km $a = 10$ km, $b = 0.5$ km along 42°S
- (c) 25 February 1970 . $L = 20.4$ km. $a = 10$ km, $b = 0.6$ km along 43°S .
- (d) 6 January 1971, $L = 20.3$ km, $a = 10$ km, $b = 0.6$ km, along 43°S
- (e) 2 February 1971, $L = 31.4$ km, $a = 13$ km, $b = 0.7$ km along 43.5°S

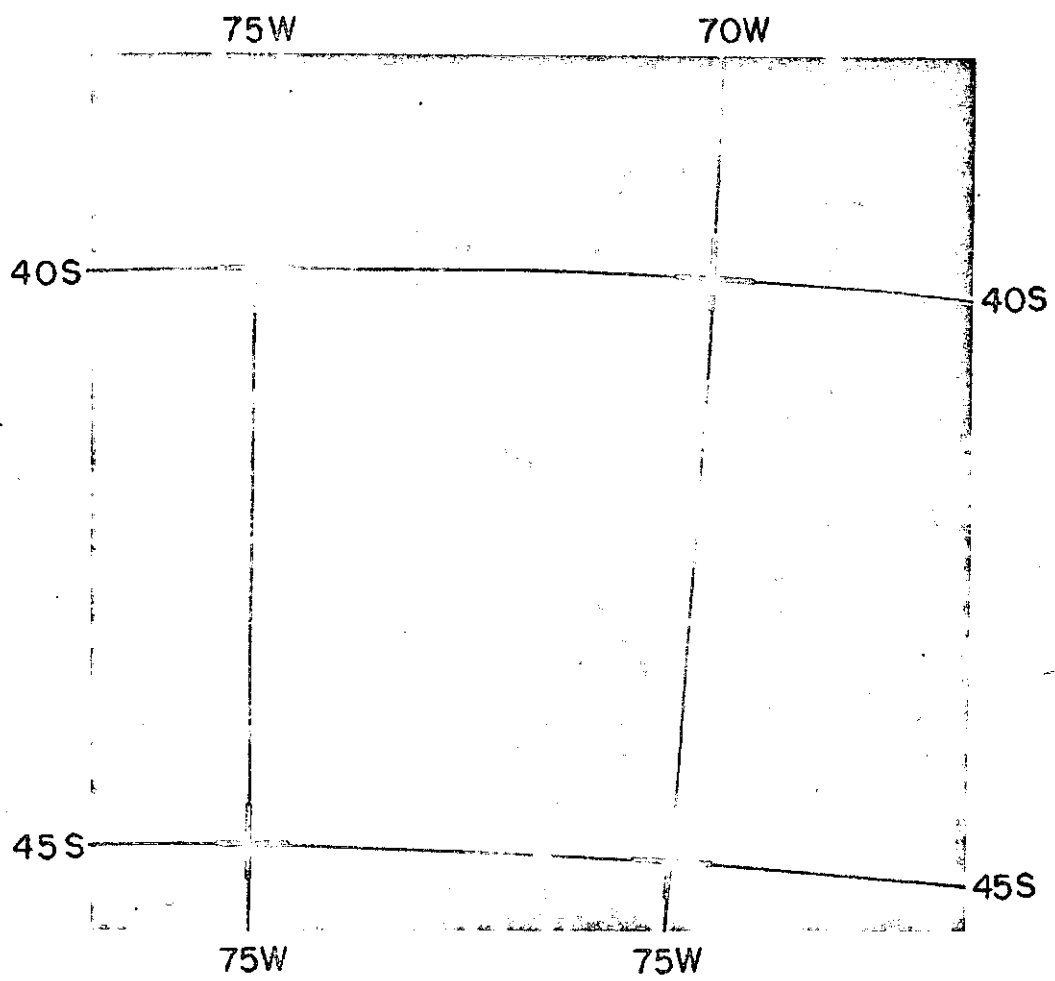
T A B L E I

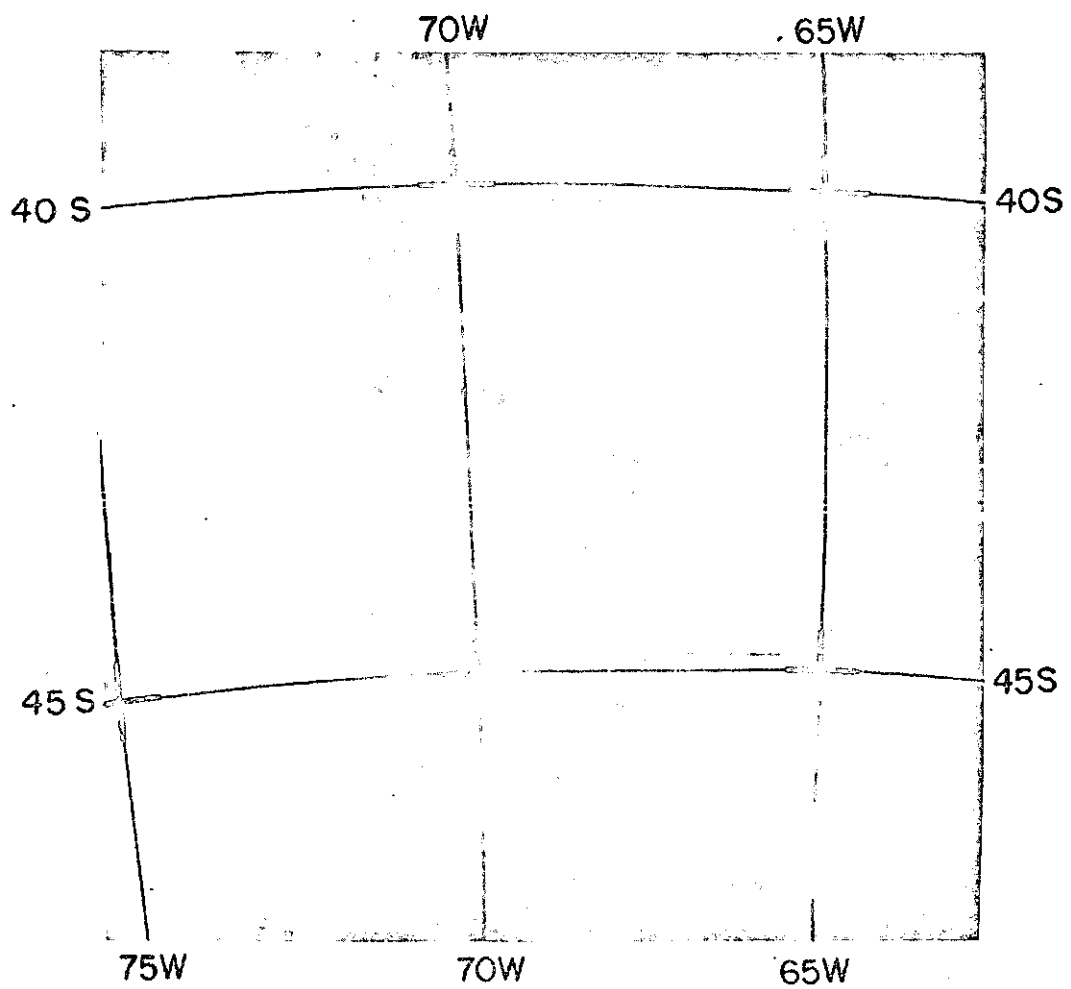
Case no	Date	Time (GMT)		Location	(km) Observed Wavelength		Computed Wavelength (km)		Mountain Profile (km) h, a, b	Max Vertical Velocity m sec ⁻¹
		Heliosync.	Geo		Heliosync.	Geosynchr.	Analytical	Numerical		
1	1 JAN. 71	ITOS 1 20:06:59 Orbit 4295	ATS 3 12:08	69°-72°W 47°-49°S	20.0	18.0	21.0 7.4 4.0	19.1 7.1 3.4	.75 10 .6	1.4
2	12 DEC. 70	ITOS 1 20:30:30 Orbit 4045	ATS 3 15:20	68°-72°W 41.5°-42.5°S	18.2	17.0	20.0 8.5	18.0 10.0	10 10 .5	0.8
3	25 FEB. 70	NIMBUS 3 16:16:00	-	66°-72°W 40°-46°S	19.8	-	-	20.4 8.1	.9 10 .6	1.1
4	6 JAN. 71	ITOS 1 20:59:25 Orbit 4358	ATS 3 13:45	70°-72°W 42°-44°S	20.1	19.2	-	20.3 11.2	.9 10 .6	2.1
5	2 FEB. 71	ITOS 1 21:24:22 Orbit 4696	ATS 3 13:07	67°-70°W 42.5°S-44.5°S	28.8	24.5	32.0 13.4	31.4 15.3	.8 13 .7	5.2

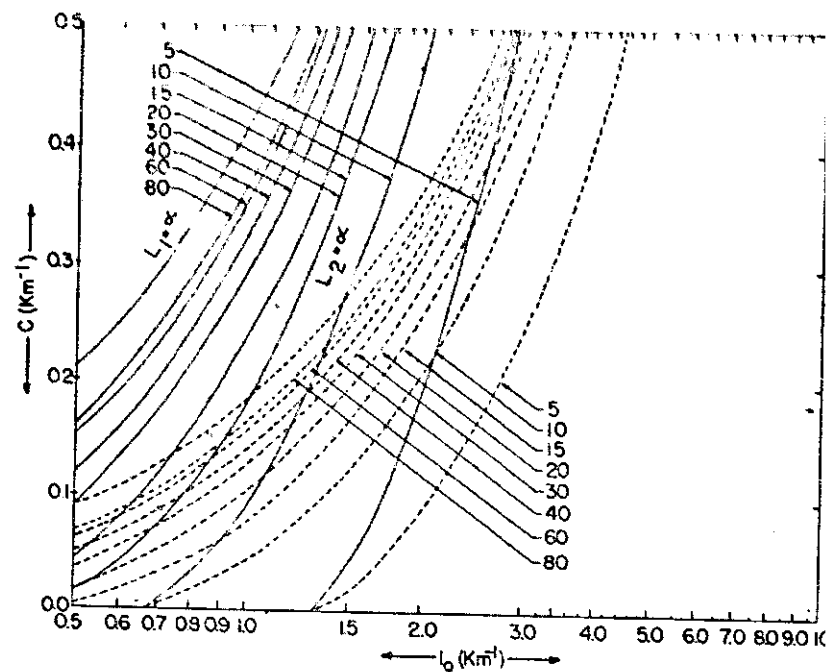




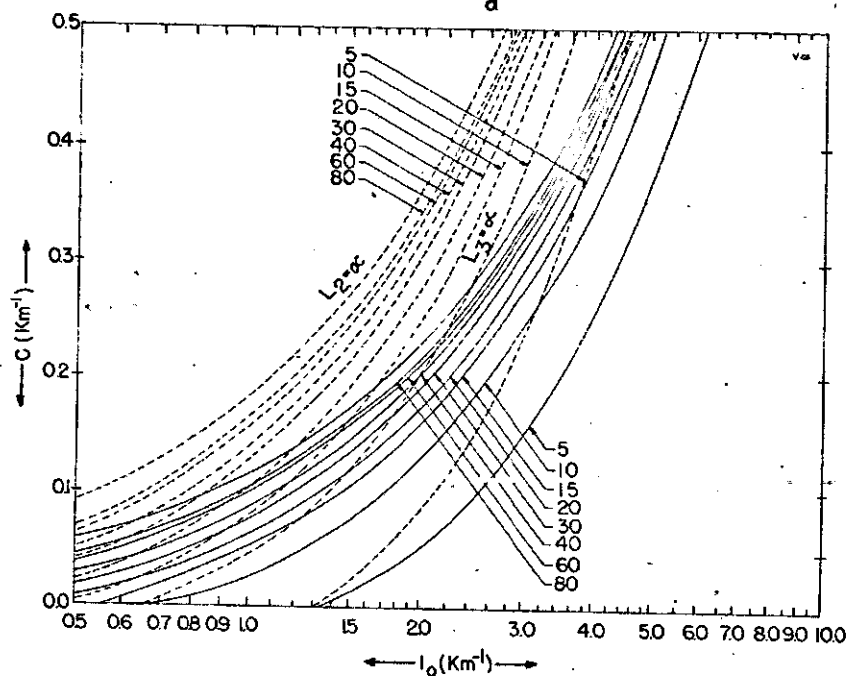




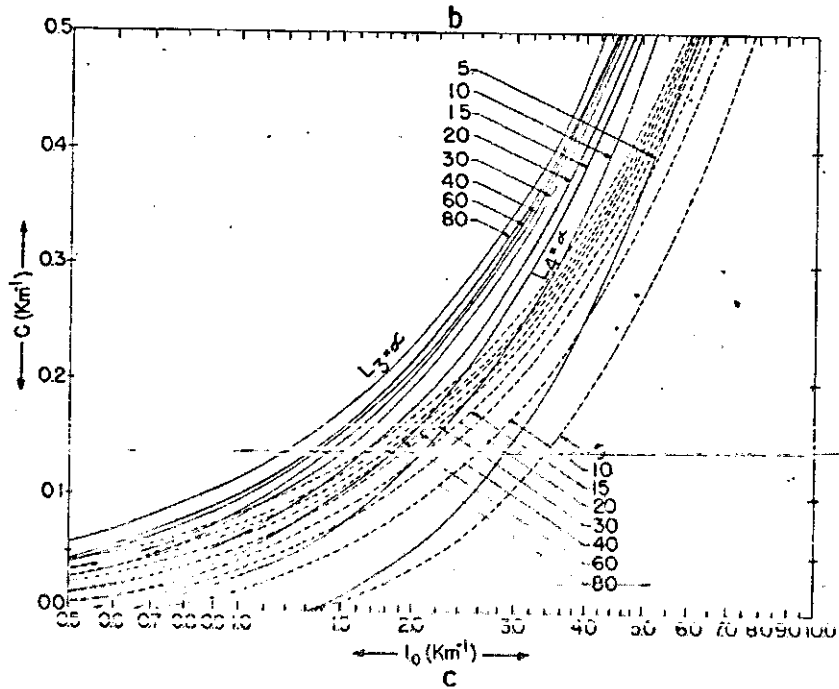




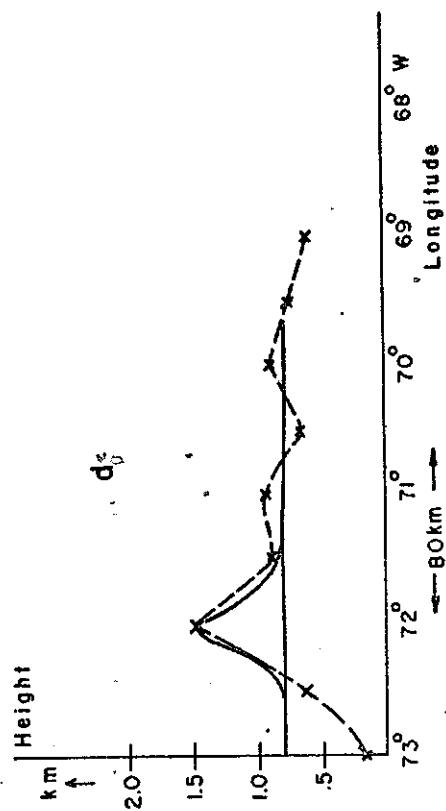
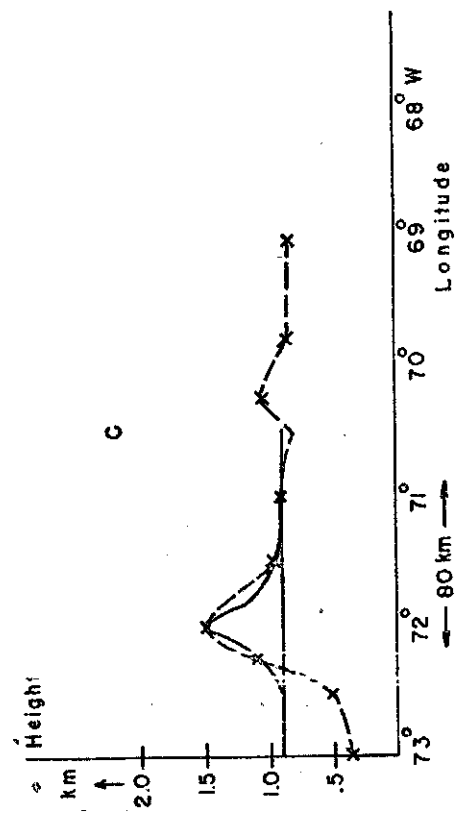
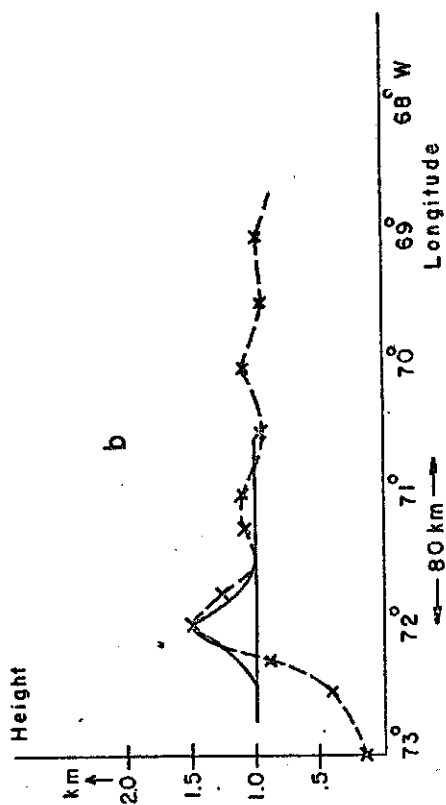
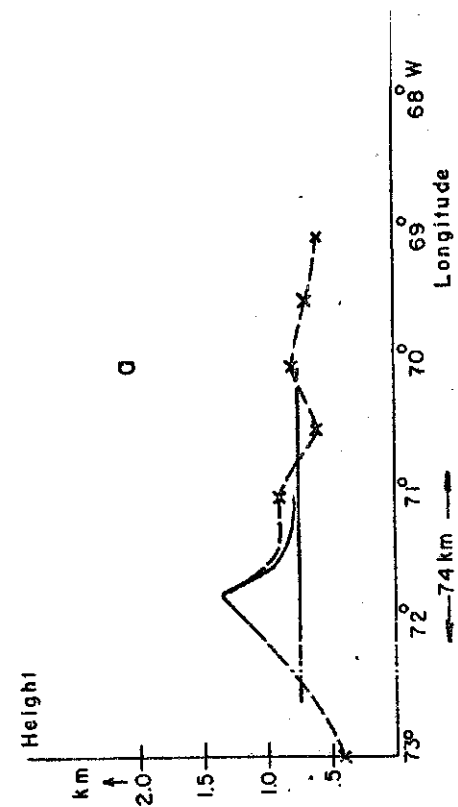
a

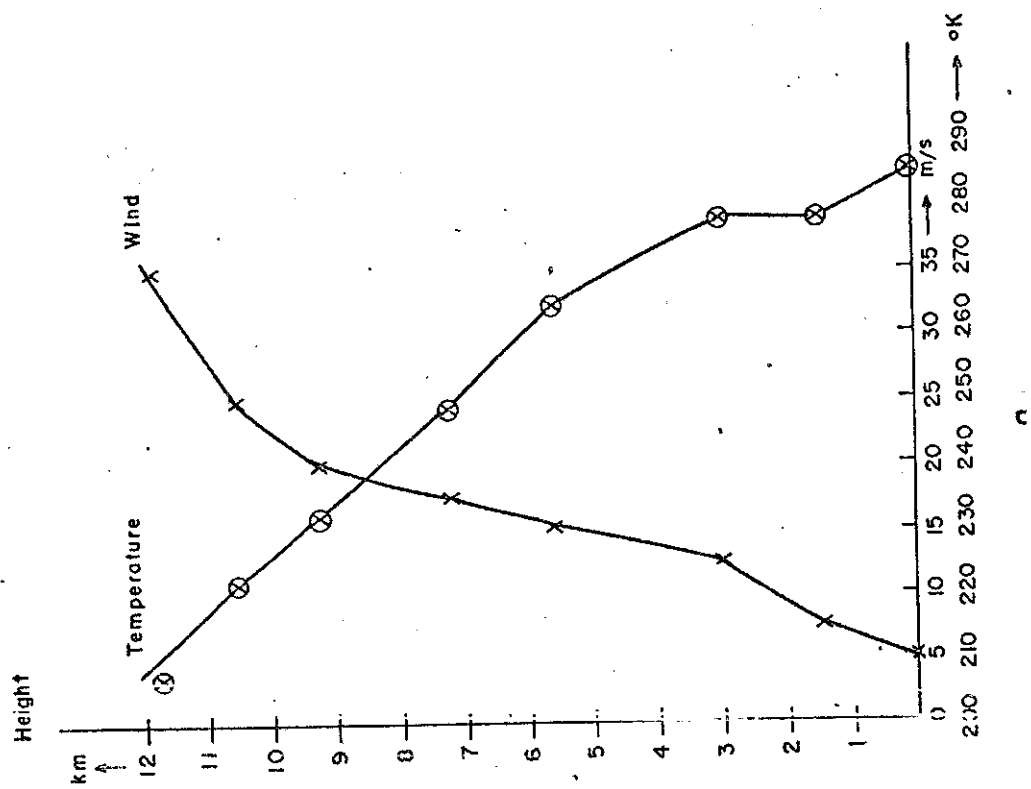
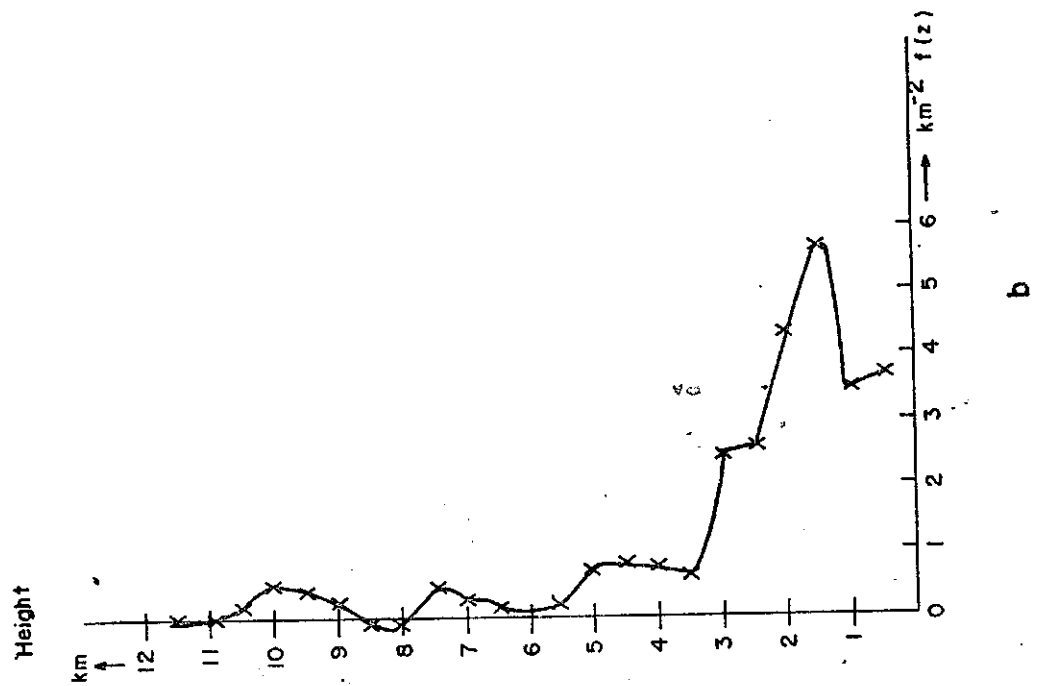


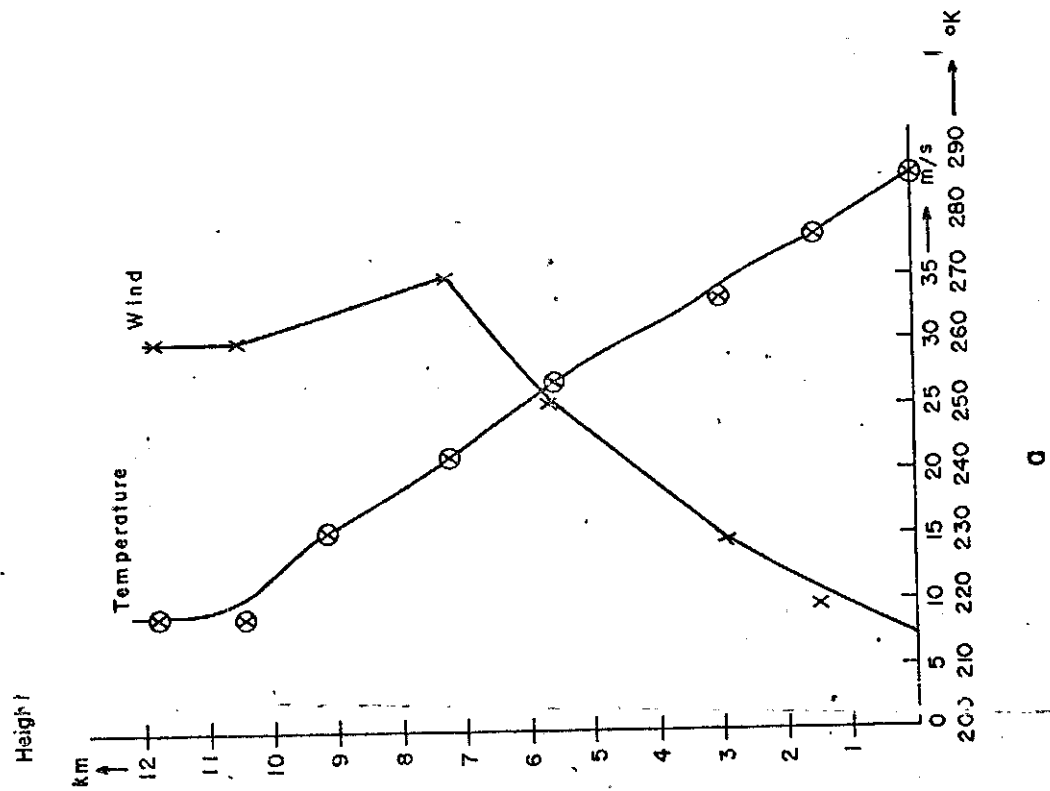
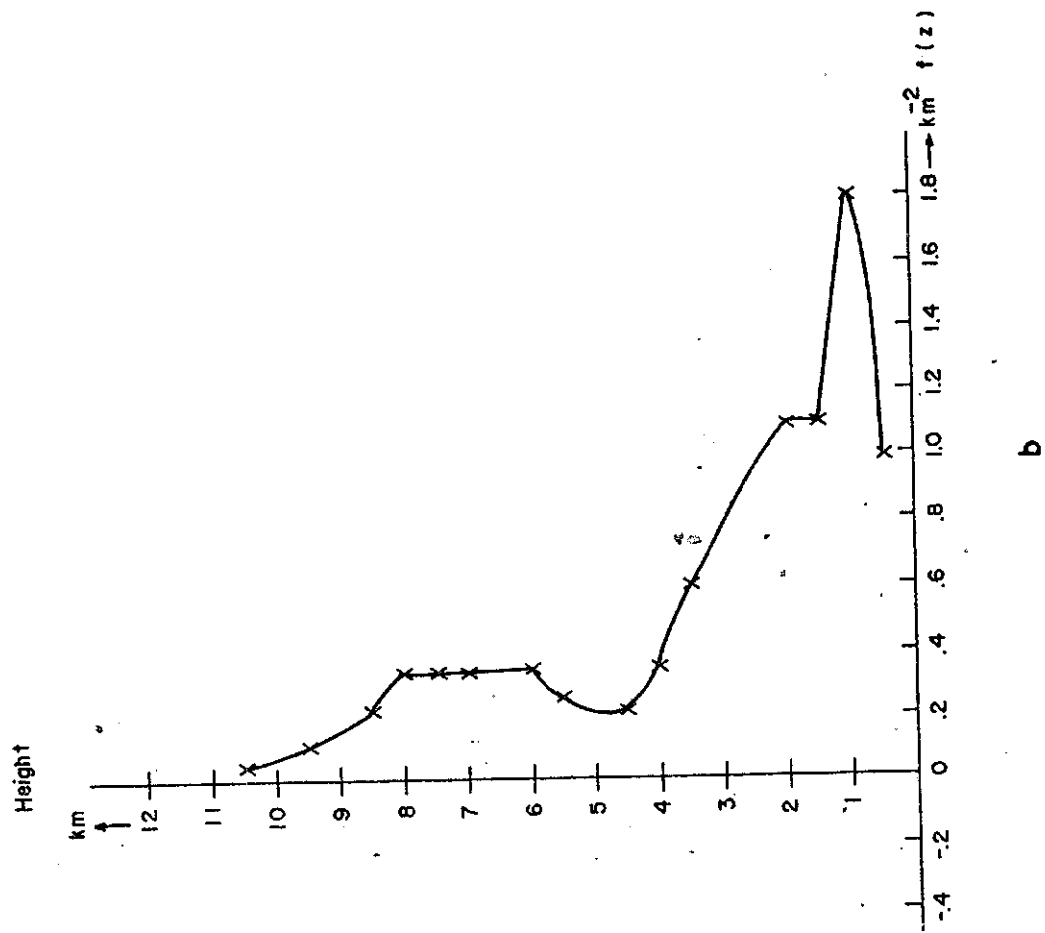
b

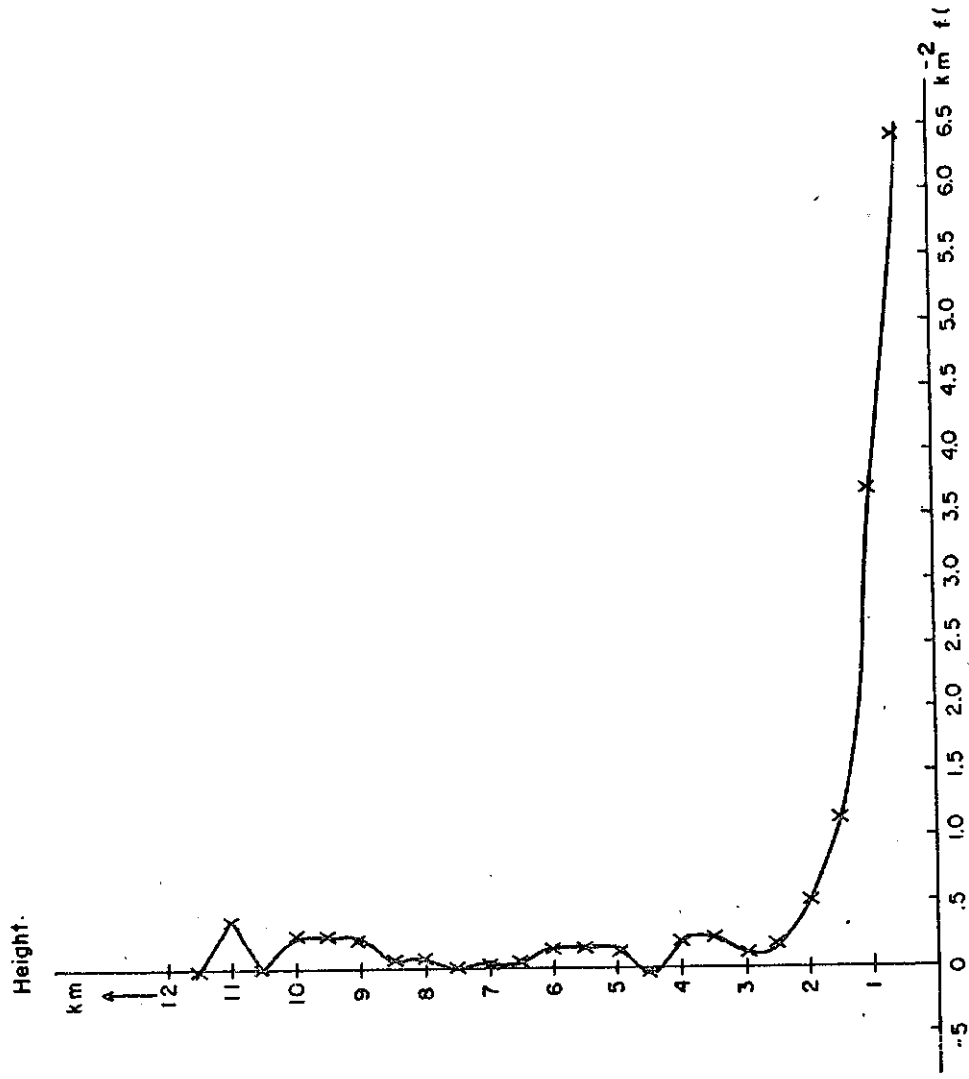


c



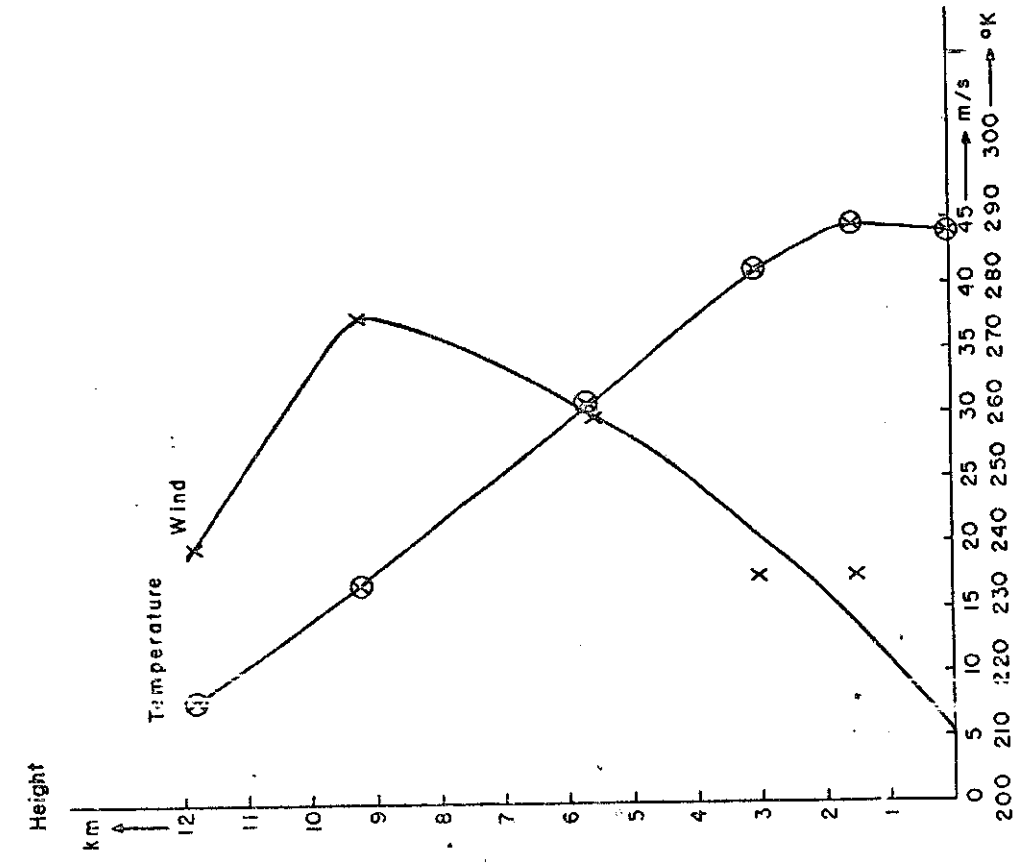




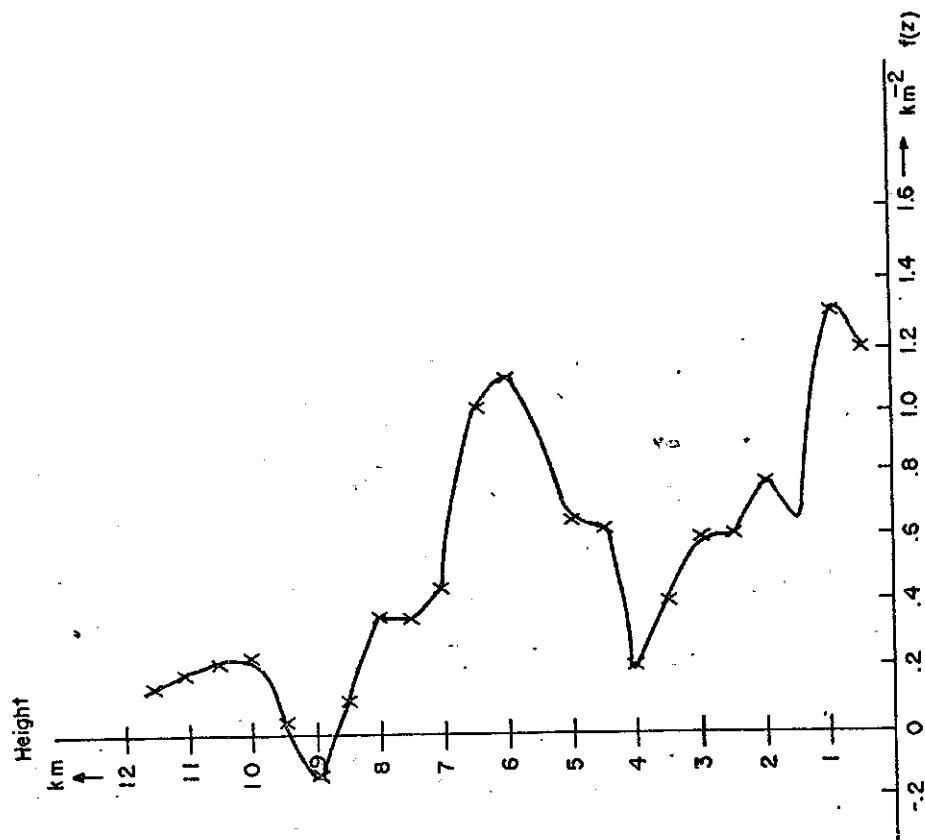


a

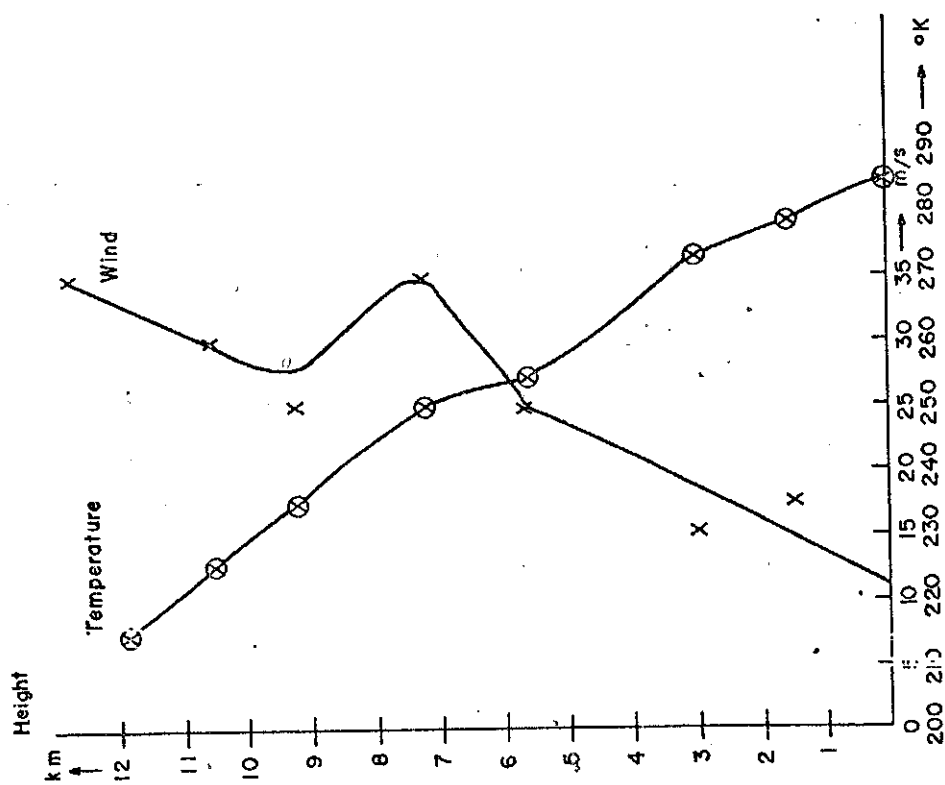
10



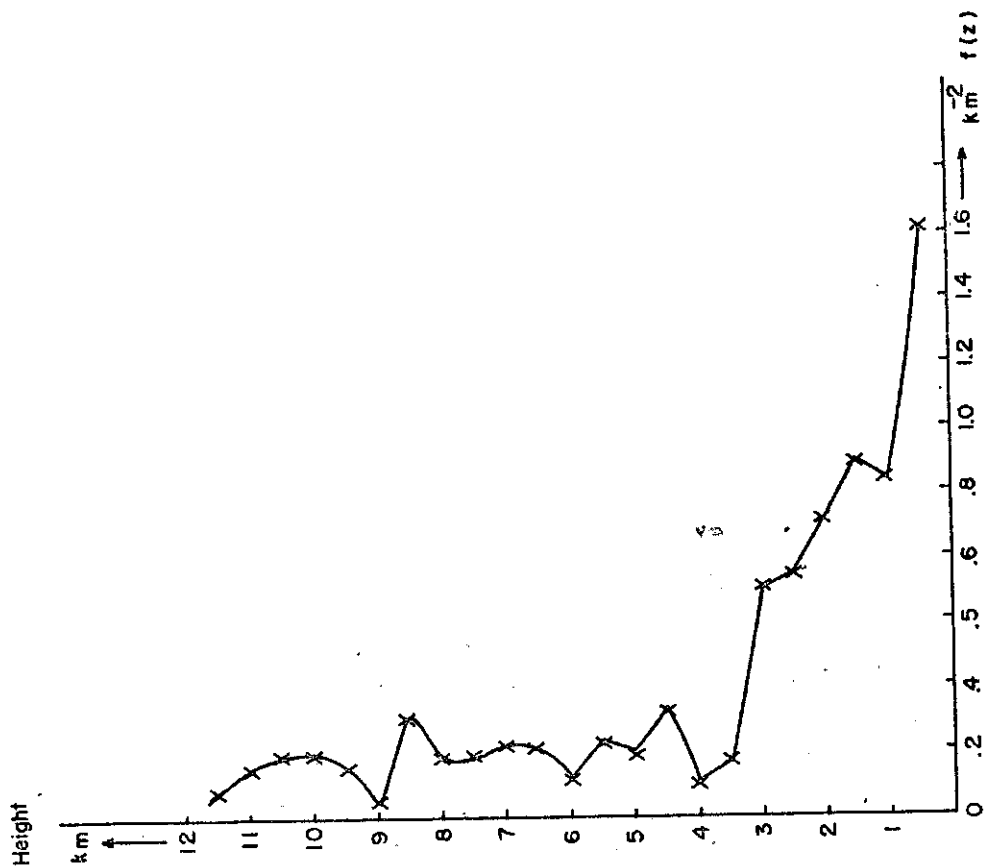
b



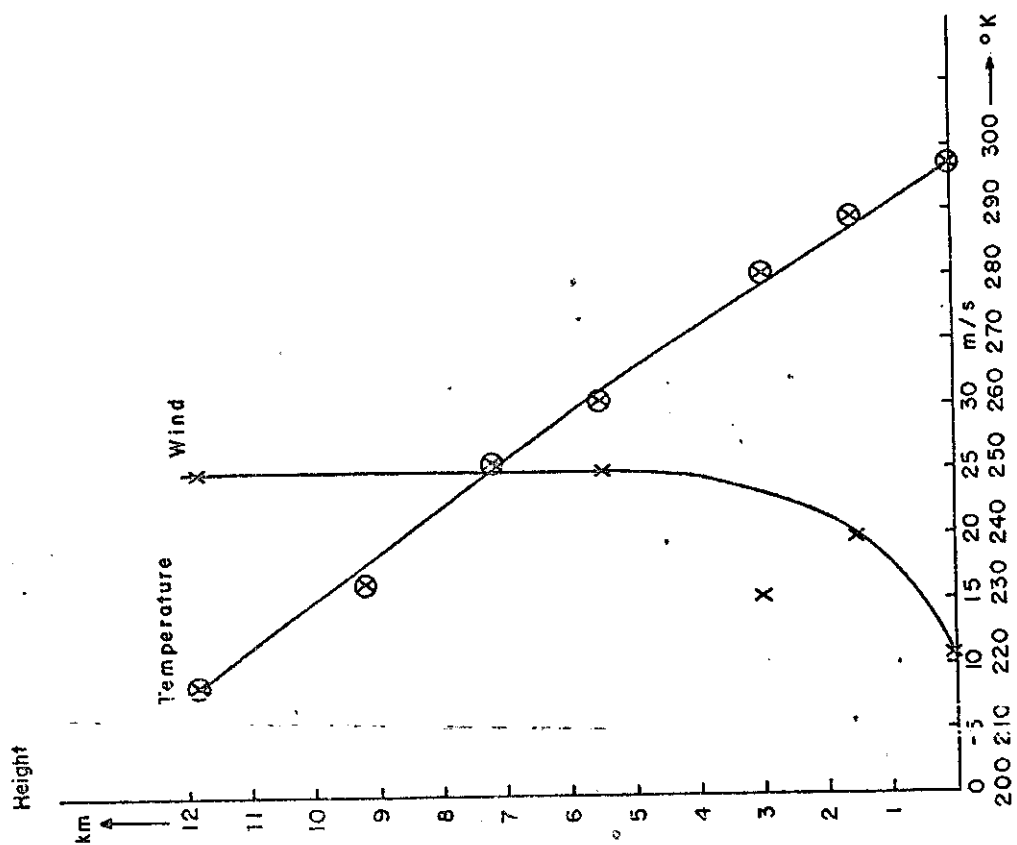
b



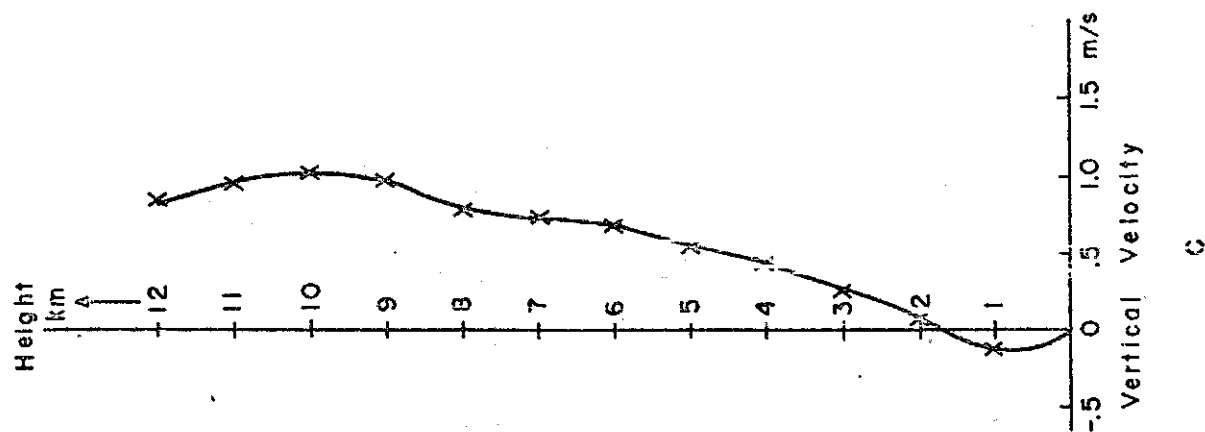
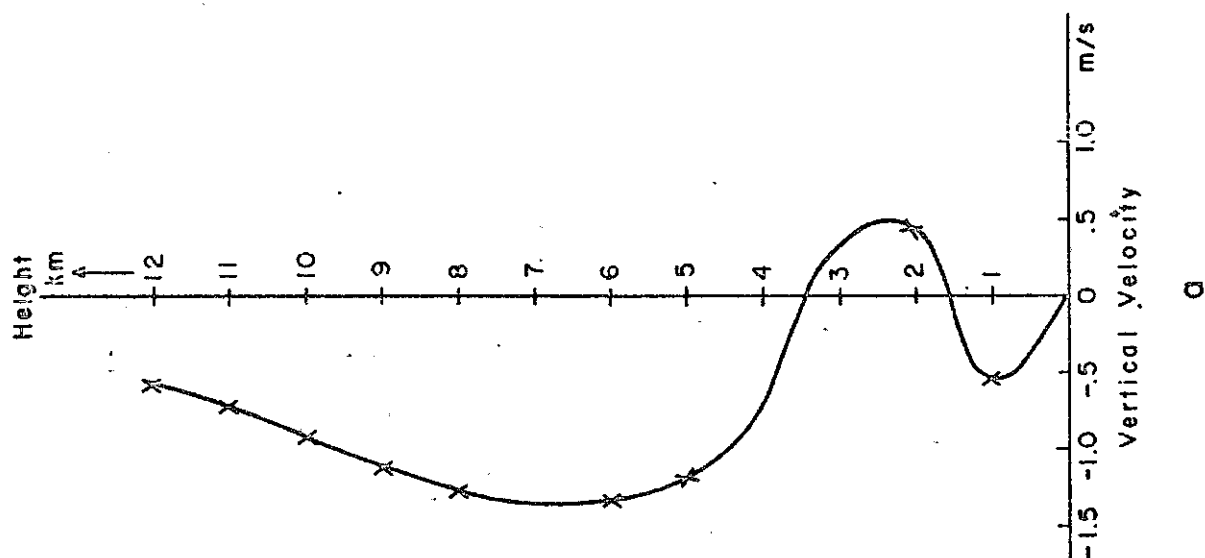
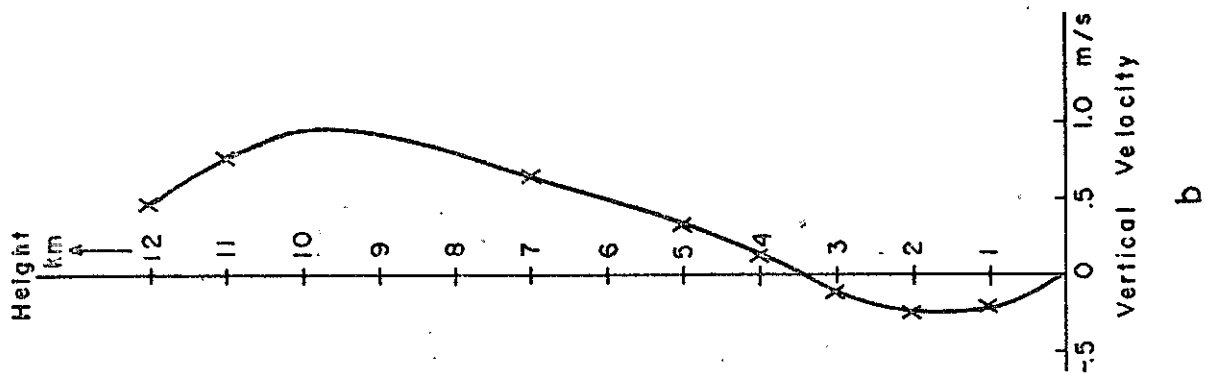
d

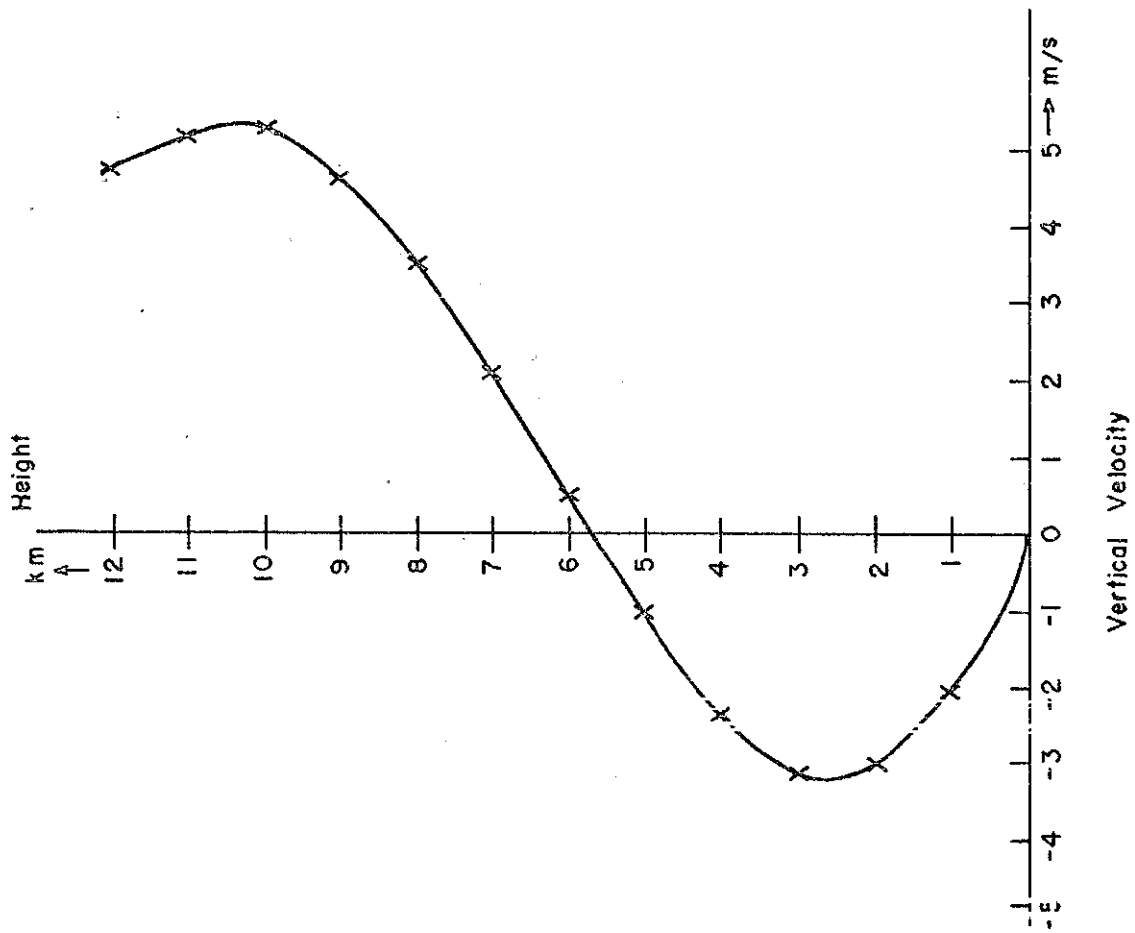


b

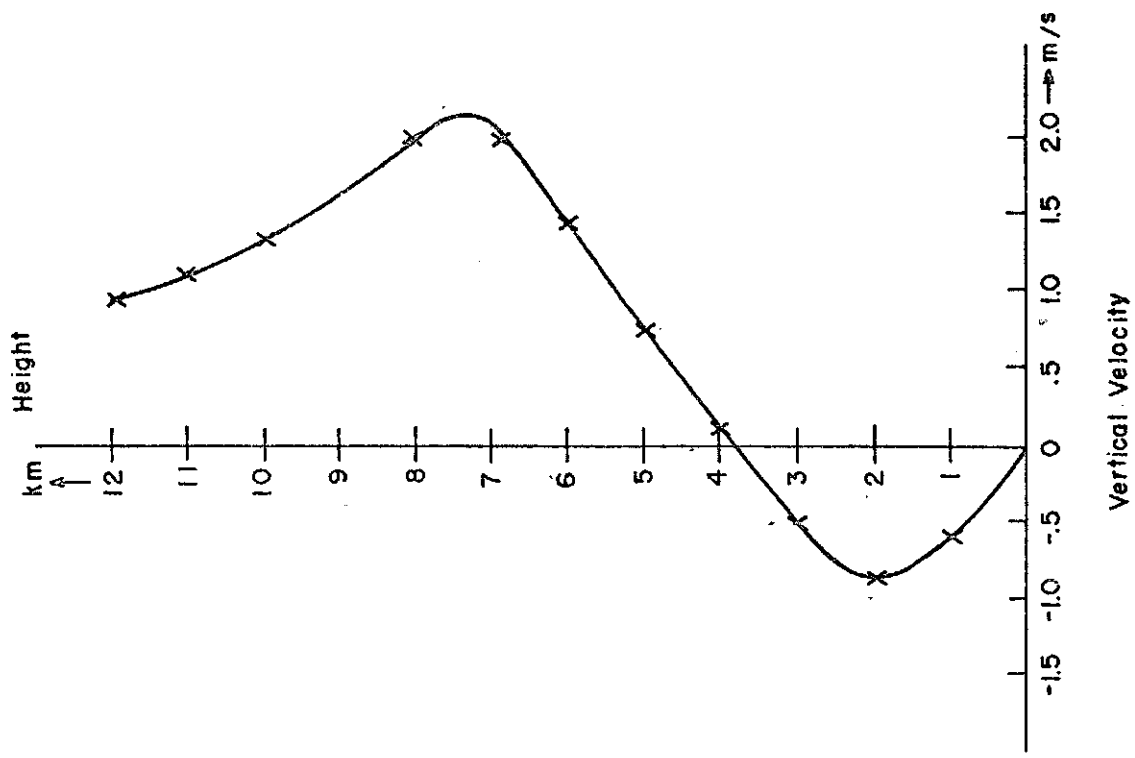


a





e



d